Numerical Analysis of a New Polymer Photonic Crystal Fiber for Sensing Applications

Issam Haddouche and Linda Cherby
Institute of Electronics and Computer Ingeneering, USTHB University, Bab Ezzouar, Algeria

Keywords: Photonic Crystal Fiber, Optical Biosensors, Polymer, Vectorial Finite Element Method.

Abstract: In this paper a new sensor design based on the enhancement of the evanescent field of the propagating modes is presented, the sensor is a modified Photonic Crystal Fiber (PCF) with Teflon AF used as a background material. Assessment of the sensor's performance is made by calculating Confinement loss of the waveguide. Full-Vector Finite Element Method is used throughout the analysis. Results show a remarkable enhancement in the evanescent field for this sensor compared with standard PCF waveguide.

1 INTRODUCTION

Over the Past decade, Photonic Crystal Fibers (PCF) technology earned more attention in sensing applications, Biosensing in particular (Mescia et al., 2009; Coscelli et al., 2010). PCFs offer more design flexibility, remote sensing and the possibility of greater wave field profile control thanks to the various geometry parameters, they also possess a wide single-mode operating wavelength range and a very interesting light dispersion properties (Saitoh and Koshiba, 2002).

Comparing with conventional Teflon, Teflon AF has a very interesting feature, that is, light transmission at infrared and visible wavelength regions with relatively low refractive index (Yang et al., 2008).

The design of this sensor is characterized by the intensity of the evanescent part of the optical field, i.e. the propagating mode inside the fiber can interact with the outer medium (Yin et al., 2008), and thus any disturbance in this last can be detected, which is a very interesting feature in chemical and Bio-sensing.

The evanescent optical power is evaluated by calculating Confinement loss of the waveguide.

A full-vector analysis is critical in order to get accurate and reliable results (Saitoh and Koshiba, 2002). FV-FEM was used throughout this study with edge/nodal triangular elements (Koshiba et al., 1994) (Koshiba and Tsuji, 2000).

In this work the performance of a Teflon AF PCF based sensor is evaluated by calculating Confinement loss (Cl) using a FV-FEM and a perfectly matched layer (PML) as boundary condition (Berenger, 1993).

2 DESCRIPTION OF THE MODEL

We consider in figure 1 a PCF with two rings of air holes surrounded by a rectangular PML, with the hole pitch denoted Λ, hole diameter of the inner ring d and that of the outer ring d1. From Maxwell's equation the following vectorial wave equation is derived (Saitoh et al., 2003):

$$\nabla \times ([s]^{-1}\nabla \times \boldsymbol{E}) - k_0^2 n^2 [s]\, \boldsymbol{E} = 0 \qquad (1)$$

where $\boldsymbol{E}$ is the electric field, $k_0=2\pi/\lambda$ is the free space wavenumber, λ is the wavelength, n is the refractive index, [s] is complex and depends on s_i (i = 1...4) inside the PML region and equals the identity matrix elsewhere (Saitoh et al., 2003):

$$[s] = \begin{bmatrix} s_y/s_x & 0 & 0 \\ 0 & s_x/s_y & 0 \\ 0 & 0 & s_x s_y \end{bmatrix} \qquad (2)$$

s_x and s_y are given in table 1 for each PML region with:

$$s_i = 1 - j\alpha_i \left(\frac{\rho}{t_i}\right)^2 \qquad (3)$$

where i refers to zone 1...4 in the PML region, α_i is directly related to electrical conductivity and

Table 1: PML parameters.

PML parameter	PML region							
	1	2	3	4	5	6	7	8
s_x	s_1	s_2	1	1	s_1	s_2	s_1	s_2
s_y	1	1	s_3	s_4	s_3	s_3	s_4	s_4

reflection coefficient (Viale et al., 2005), ρ is the distance from the beginning of the PML and t_i is thickness of the PML layer.

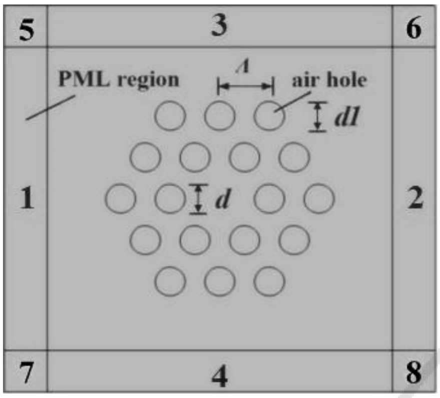

Figure 1: PCF surrounded by rectangular PML.

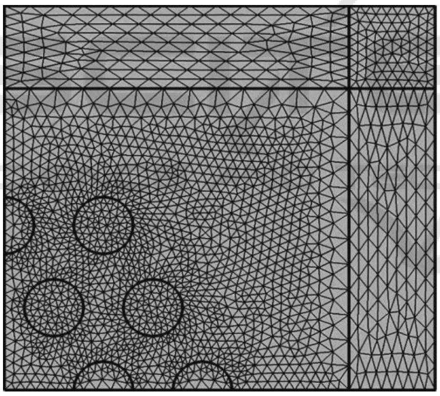

Figure 2: Computational window with meshing.

Taking advantage of the model's symmetry only one quarter is discretised into edge/nodal elements as illustrated in figure 2, which saves some computation time, memory and enhances accuracy.

The following eigenvalue equation is derived (Koshiba and Tsuji, 2000):

$$[K]\{E\} - (k_0 n_{eff})^2 [M]\{E\} = 0 \tag{4}$$

where [K] and [M] are the FEM global matrices, n_{eff} is the effective index of the propagating modes.

The PML layer will be used to calculate the confinement loss [dB/m] of the propagating modes using the following relation (Saitoh et al., 2003):

$$Cl = 8.686\, Im[k_0 n_{eff}] \tag{5}$$

Im stands for imaginary part.

Refractive indices of silica and Teflon AF are modeled using Sellmeier equation (Yang et al., 2008) (Paschotta).

$$n(\lambda)^2 = 1 + \frac{B_1\lambda^2}{\lambda^2 - C_1} + \frac{B_2\lambda^2}{\lambda^2 - C_2} + \frac{B_3\lambda^2}{\lambda^2 - C_3} \tag{6}$$

The values of B_i and C_i are summarized in table 2.

Material Dispersion of silica and Teflon AF are illustrated in figure 3.

Table 2: Sellmeier Equation parameters.

material	B_1	C_1	B_2	C_2	B_3	C_3
Silica	0.696	0.005	0.4	0.0135	0.897	97.93
Teflon AF	0.181	0.014	1	159.28	0	0

3 RESULTS AND DISCUSSION

The confinement loss is calculated for two kinds of PCF, the first PCF (conventional PCF) has d1=d=1.38 µm however the second PCF (modified PCF) differs from the first in that d1 is smaller than d, each waveguide is modelled for the two background materials silica and Teflon AF.

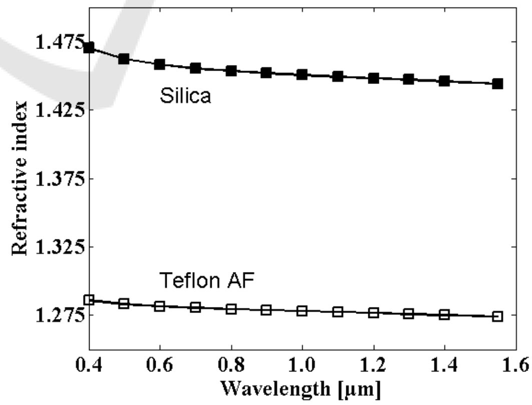

Figure 3: Material dispersion of silica and Teflon AF.

Figures 4 and 5 depict the x-component of the electric field of the HE_{11}^{x} mode of the Teflon AF PCF for the two PCF models.

The mode field profile seems to be more extended outside the core in the modified PCF, this is due to the fact that the hole diameter of the outer ring is smaller thus enhancing the evanescent field.

After solving eigenvalue equation (4), complex n_{eff} is obtained and relation (5) is used to calculate confinement loss.

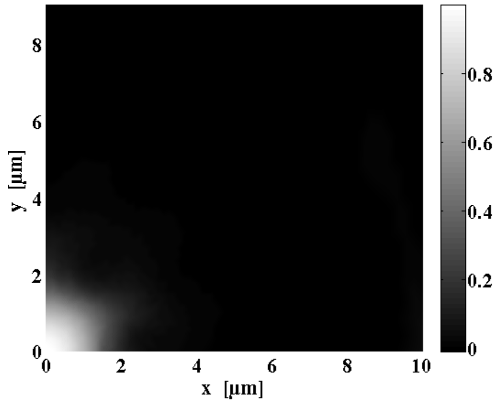

Figure 4: x-component of the electric field of the HE_{11}^{x} mode of the Teflon AF conventional PCF with: 18 air holes, Λ=2.3µm and d=d1=1.38µm.

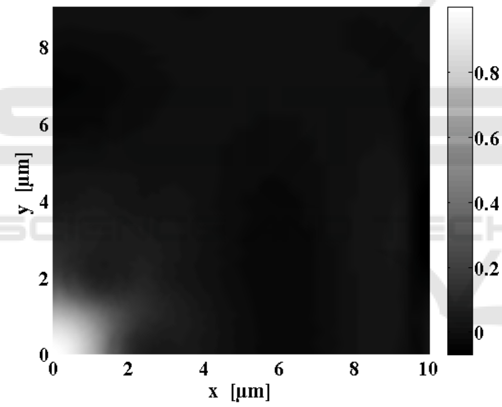

Figure 5: x-component of the electric field of the HE_{11}^{x} mode for the modified Teflon AF PCF with: 18 air holes, Λ=2.3µm, d= 1.38µm and d1=0.92µm.

Numerical Results are illustrated in figures 6 and 7, where confinement loss of the HE_{11}^{x} mode was calculated with respect to wavelength for conventional and modified two rings PCFs respectively and for two background materials. The hole diameter of the outer ring was taken d1=0.92µm in the modified PCF.

These results show that confinement loss increases with wavelength, this can be explained by the dependence of the mode field diameter (MFD) on wavelength (Saitoh and Koshiba, 2005) (Agrawal, 2002) i.e. the more MFD is important the more mode profile is extended outside the core. We can also note that Teflon AF PCF has a greater confinement loss than that of silica PCF, this is due to the lower index contrast in Teflon case providing wider MFD (Saitoh and Koshiba, 2005) (Agrawal, 2002).

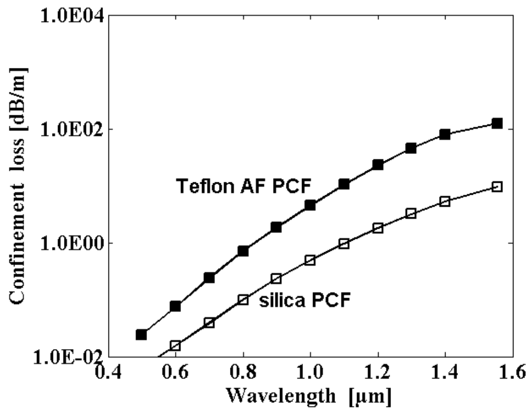

Figure 6: Confinement loss plot of conventional PCF with respect to wavelength with: 18 air holes, Λ=2.3µm, d=1.38µm and d1=d.

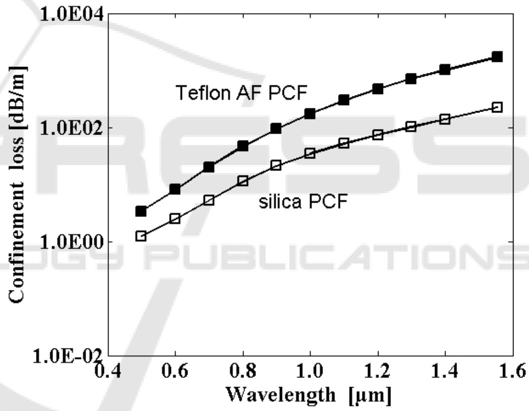

Figure 7: Confinement loss plot of modified PCF with respect to wavelength with: 18 air holes, Λ=2.3µm, d=1.38µm and d1=0.92µm.

Reducing the hole diameter of the outer ring d1, allows more energy to leave the core towards the outer medium this is the reason why confinement loss is more important in the modified PCF as illustrated in figure 7.

4 CONCLUSIONS

A numerical study of a PCF for Biosensing applications was presented in this paper, propagation loss is a very important parameter in evanescent wave based sensors, these sensors are simple, cheap and easy to use unlike other types such as Surface

Plasmon Resonance (SPR) based sensors, and can be used within interferometers to detect phase shift resulting from disturbance in outer medium. As it is well known PCFs are inherently lossy, the use of some special materials with lower refractive indices than silica such as Teflon AF will increase confinement loss even more because of the lower index contrast between the core and the cladding, altering geometrical parameters values such as the pitch Λ and the hole diameter d can also increase confinement loss.

REFERENCES

L. Mescia, F. Prudenzano, L. Allegretti, 2009. *Design of silica based photonic crystal fiber for biosensing applications*, Journal of Non-Crystalline Solids 355.

Coscelli, E, M. Sozzi, F. Poli, 2010. *Toward A Highly Specific DNA Biosensor: PNA-Modified Suspended-Core Photonic Crystal Fibers*, IEEE Journal of Quantum Electronics, Vol. 16, No. 4, 967–972.

Saitoh, K, M. Koshiba, 2002. *Full-vectorial imaginary-distance beam propagation method*, IEEE Journal of Quantum Electronics, Vol. 38, No. 7, 927–933.

Yang, M. K., R. H. French, E. W. Tokarsky, 2008. *Optical properties of Teflon® AF amorphous fluoropolymers, J. Micro/Nanolith. MEMS MOEMS*, Vol. 7, No. 3, 1–9.

S. Yin, C. Zhan, P. Ruffin, 2008. *Fiber optic sensors*.

Koshiba, M, S. Maruyama, K. Hirayama, 1994. *A vector finite element method with the high-order mixed-interpolation-type triangular elements*, Journal of lightwave technology, Vol. 12, No. 3, 495–502.

Koshiba, M, Y. Tsuji, 2000. *Curvilinear hybrid edge/nodal elements with triangular shape for guided-wave problems*, Journal of lightwave technology, Vol. 18, No. 5, 737–743.

Berenger, J., 1993. *A perfectly matched layer for the absorption of Electromagnetic waves*, Journal of computational physics, Vol. 114, 185–200.

Saitoh, K, M. Koshiba, T. Hasegawa, E. Sasaoka, 2003. *Chromatic dispersion control in photonic crystal fibers: application to ultra-flattened dispersion*, Optics express, Vol. 11, No. 8, 843–852.

Viale, P, S. Février, F. Gérome, H. Vilard, 2005. *Confinement Loss Computations in Photonic Crystal Fibres using a Novel Perfectly Matched Layer Design*, COMSOL Multiphysics User's Conference Paris.

R. Paschotta, Sellmeier Formula, RP Photonics, *https://www.rp-photonics.com/sellmeier_formula.html*.

Saitoh, K, M. Koshiba, 2005.*Numerical Modeling of Photonic Crystal Fibers*, Journal Of Lightwave Technology, Vol. 23, No. 11, 3580- 3590, November.

G. P. Agrawal, 2002. *Fiber-Optic Communications Systems*, Third Edition, Wiley, pp. 33-37.